3D Numerical Simulation on Disk Type RDE used Hydrogen-Air Premixed Gas and Non-premixed Gas with Multi-Ports Injection: Relation between injection mode and flame index

Takumi Ito, Nobuyuki Tsuboi and Kohei Ozawa
Kyushu Institute of Technology
Kitakyushu, Fukuoka, 804-8550, Japan

A. Koichi Hayashi
Aoyama Gakuin University
Shibuya, Tokyo, 150-8366, Japan

1 Introduction

Research has been performed to utilize the enormous energy of detonation phenomena in gas turbine engines and rocket engines. The two most representative types of detonation engines are (ⅰ) the pulse detonation engine (PDE), which produces thrust by intermittent detonation, and (ⅱ) the rotating detonation engine (RDE), which produces thrust at high frequencies by propagating detonation in the circumferential direction inside the combustor. In an attempt to use turbines in detonation engines, a study combining a PDE with a turbine was reported by Schauer et al [1] in 2003. Subsequently, in 2017, Naples et al [2] conducted experiments combining turbines with RDEs and reported improved turbine efficiency; in 2018, Huff et al [3, 4] reported the use of a radial turbine in RDEs instead of the axial flow turbine used in the previous studies in the disk-type rotating detonation engine (DRDE) were proposed by Huff et al [3, 4]. The use of a radial turbine instead of an axial turbine is expected to increase the expansion ratio per stage and achieve higher efficiency. However, the detailed flow field structure inside a DRDE combustor is not understood at present. Understanding this structure is essential for the practical application of DRDE and its use in design. Recently, pressure gains have been attracting attention. Pressure drop and backflow due to injection are being studied [5].

In this study, we understand the propagation mechanism in a DRDE combustor by 3D numerical simulations to find how the propagation mechanism changes depending on the injection method and whether it is a non-premix or premix injection system.

Correspondence to: ito.takumi578@mail.kyutech.jp

2 Numerical Method

In the present study, the three-dimensional compressible Navier-Stokes equations with detailed chemical reactions are used as the governing equations. The chemical reaction model is the UT-JAXA model [6] with 9 chemical species (H_2, O_2, O, H, OH, HO_2, H_2O_2, H_2O, N_2) and 21 elementary reactions, corresponding to the high temperature and high-pressure combustion model. This model includes many high-pressure-dependent three-body reactions. The semi-implicit technique is employed to treat the production term implicitly and the remaining terms explicitly, and the second-order accurate MUSCL [7] method is used for the convection term in the HLLC/LLF [8]. The point implicit is used for the integration of the source term. A three-step TVD Runge-Kutta [9] method is used for the time integration term. In this study, the scale of calculation is approximately 1/2 of the experiment. Therefore, although turbulent flow appears in the combustor, a turbulence model is not used in this study due to the computational cost. The wall boundary condition was assumed to be adiabatic and slip-wall, neglecting viscous effects near the wall.

3 Simulation Conditions

The area of the 3D combustor of DRDE has the geometry shown in Fig. 1. The calculations are started by using the 1D detonation result to the ignition source region . the micro-laval nozzles are installed over the area of the outer surface of the disc combustor. The mass flow rate of the H_2/Air is varied according to its nozzle area ratio A_e/A_t and the pressure ratio between the inside of the combustor and the storage.

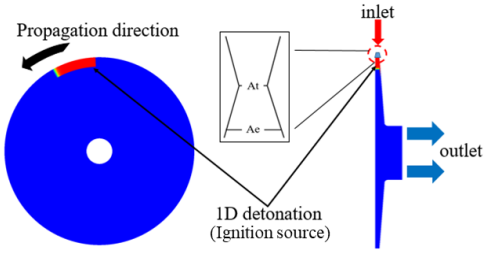

Fig .1 Injection model of DRDE.

As shown in Fig. 2, the 3D computational grid used in this study consists of three regions. The zones where the detonation waves have a particularly fine grid. The physical values in the overlapped region between the different grids are calculated by the interpolation coefficients. The number of grid points for each zone is shown in Table 1.

Table 2 shows the numerical initial conditions. In the present analysis, two injection cases are compared: Case 1 is non-premix, and Case 2 is premix injections, respectively. Stagnation pressure is 0.4 MPa. The nozzle area ratio is 2.5. The mass flow rate and oxidizer injection area vary from the case to case. Figure 3 shows a schematic diagram of each injection cases. The colors of each port and slit indicate the type of injected gas. Blue, red, and purple indicate air, H_2, and H_2/Air mixture , respectively. It can be said that Case 1 is a simple representation of cross-flow, in which the oxidizer is injected from the slit and the fuel is injected from the port, which is often used in DRDE and RDE injection.

Table 1. Present computational grid systems.

Zone	1	2	3
Grid dimension (i×j×k)	81x21x601	204x21x131	110x99x71
	2,356,695 points		

(a) Front of DRDE grid. (b) Side of DRDE grid.

Fig. 2 Computational grids (Three zones).

Table 2. Numerical initial conditions

Case	Injection method	Stagnation condition	Ambient condition	Nozzle area ratio(*Ae*/*At*)	Mass flow rate [g/s]	Area of air injection[mm^2]
1	Non-premix	0.4 [MPa] 300 [K]	0.1 [MPa] 300 [K]	2.5	230	76.1
2	Premix				229	60.5

Case1 Case2

Fig.3 Schematic diagram of injection gases and shapes. blue: oxidant, red: H2, purple: H2-air premix gas.

4 Results and Discussion

Comparison of Case 1 and Case 2 for propagation transition, time-average field flow field, and pressure gain.

4-1 Comparison of propagation transition

Figure 4 shows the temperature contours of the instantaneous field for case 1 and case 2. In Case 1, although a clear plane wave is not generated, a small area on the outer surface contains a high-temperature and high-pressure region. In Case 2, the shape of the rotating detonation wave is flat, and a high-temperature region is also observed in the oblique shock wave area on the radial side. The detonation propagation velocity calculated by pressure history is shown in Fig. 5. It is overdriven in both cases, and the reason for this is that the geometry of the DRDE causes the shock waves to impinge on curved walls, and the overlapping of the shock waves creates a high-pressure zone on the wall surface.

Case1 (Non-premix) Case2 (Premix)

300 Temperature [k] 3300

Fig.4 Change in propagation morphology due to different injection methods.

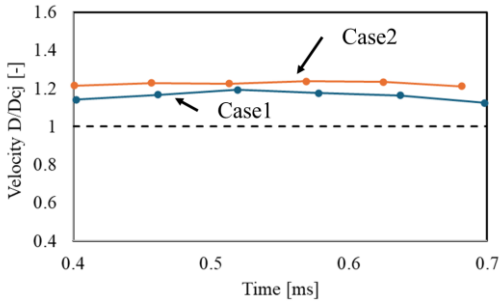

Fig.5 Detonation propagation velocity.

4-2 Comparison of time-averaged fields

The temperature contours of the time-averaged field and velocity vectors are shown in Fig. 6. The temperature of the time-averaged field is critical to understand the thermal stress in the combustor. The constant temperature distribution was found in Case 2. From this result, thermal stress can be suppressed by the injection method. In the case of non-premix, the temperature increased relatively slowly toward the outlet. The contours of heat release in the time-averaged field are shown in Fig. 7. The heat release is significantly different between non-premix and premix, which is due to the disturbance of the combustion wall surface in the case of non-premix by unburned gas pockets. The variation of pressure, temperature, density, and Mach number in the time-averaged field with flow direction is shown in Fig. 8. Non-premixed results (Case 1) in higher pressure and lower temperature compared to the premixed results(Case 2). The difference in temperature and pressure in the averaged results depends on the injection mode. We need to investigate the difference between combustion mode and injection modes. Thus, the ratio of non-premixing to premixing must be estimated using the flame index.

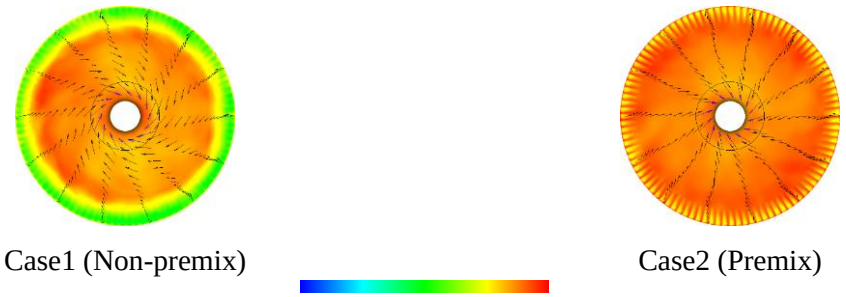

Fig.6 Temperature contours of time-averaged fields and velocity vectors.

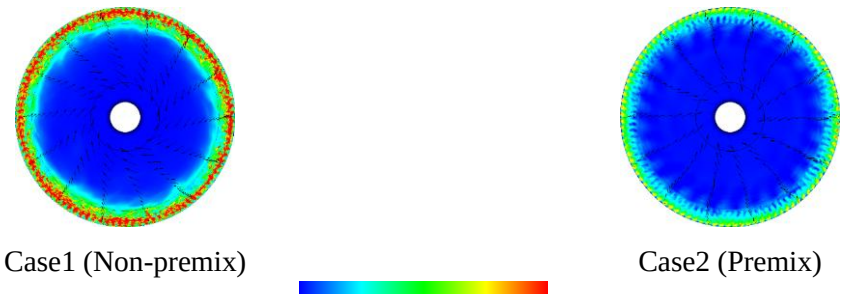

Fig.7 Contours of heat release in time-averaged fields.

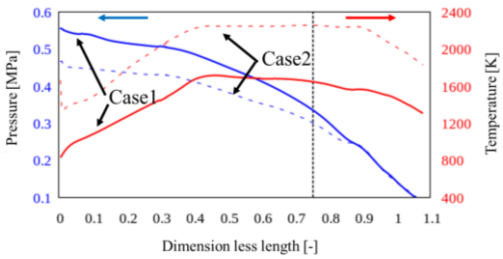

Pressure and Temperature

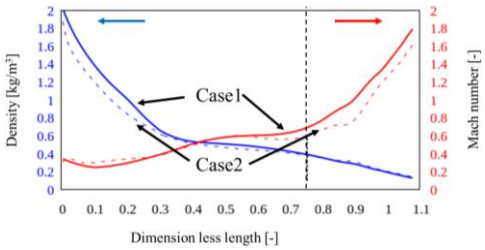

Density and Mach number

Fig.8 Variation with flow direction in time-averaged field.

4-3 Pressure gain

Pressure gain (PG) is calculated from the difference between the pressure supplied into the combustor and the pressure discharged from the combustor outlet. It is an indicator to improve energy efficiency and thrust. The definition of PG is as follows:

$$p_{t,out} = p_{s,out} \times \left(1 + \frac{r-1}{2} M_{out}^2\right)^{\frac{r}{r-1}} \quad (r = 1.25) \tag{1}$$

$$\eta = \left(p_{t,out} - p_{t,in}\right)/p_{t,in} \qquad \text{t: total, s: static, in: inlet, out: outlet} \tag{2}$$

where $p_{t,in}$ is the inlet stagnation pressure and $p_{t,out}$ is the average outlet total pressure, respectively.

Table 3 shows the PG for each case. Cases 1 and 2 show the difference between non-premix and premix. These differ by approximately 10%, indicating that the non-premix is more advantageous. A comparison was then made for the PG of DRDE and RDE with reference to Bach et al [10]. Figure 9 plots the outlet-to-manifold pressure ratio over the outlet-to-oxidant injector area ratio. The DRDE results are plotted as closed diamonds; the other plots are for RDE. As a result, DRDE has comparable performance to RDE. On the other hand, the PG is affected by the pressure loss due to boundary layer, turbulence, and separation in the region between the stagnation chamber and injection, and combustion chamber. The results obtained by Karming simulate in two dimensions and their results do not include these pressure losses [11]. Therefore, the PG in 2D tends to be overestimated compared to 3D calculations and experimental values.

Table 3 Comparison of pressure gain and number of injection ports.

Case	Injection method	Stagnation condition	No. Wave[-]	Mass flow rate [g/s]	A_{out}/A_0 [-]	PG η [-]
1	Non-premix	0.4 [MPa] 300 [K]	1	230	1.4	-0.067
2	Premix			229	1.8	-0.183

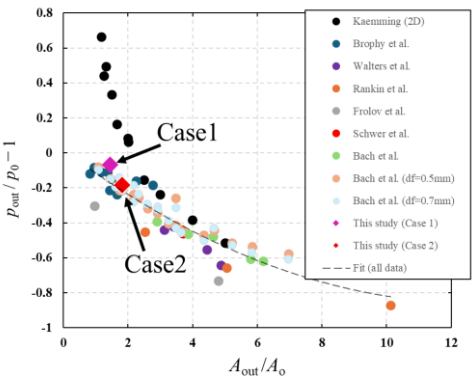

Fig. 9 Comparison of different published stagnation pressure gain data in RDEs as a function of the outlet to injector area ratio.

5 Conclusion

Three-dimensional numerical simulations on Disc-RDE are performed using the H_2/Air premix and non-premix gas detailed chemical reaction model. The conclusions are as follows:

- Due to the shape of the DRDE and the direction of detonation propagation, the reflected shock waves overlap and become high-pressure, resulting in an overdriven condition. Propagation velocity is faster in premixed injection because the propagation velocity is closer to the flame speed.
- The combustion state differs depending on the injection system, so the average temperature of the injection zone decreases, and the heat release at the detonation propagation zone increases in the case of non-premixed injection. The pressure distribution in the flow path was maintained high, which resulted in a better non-premixed injection.
- Analysis with PG showed that non-premixed injection was about 10% better than premixed injection, and comparison with RDE showed that DRDE performed as well as RDE, regardless of the injection system.

Acknowledgments

This research is conducted using SX-Aurora at the Cybermedia Center, Osaka University. The authors would like to express their gratitude to SX-Aurora.

References

[1] F. Schauer, R. Bradley, and j. Hoke, “Interaction of a Pulsed Detonation Engine with a Turbine”, 41st AIAA Aerospace Sciences Meeting & Exhibit, 6-9 Jan 2003.
[2] A. Naples, J. Hoke, R. Battelle, M. Wagner, and F. Schauer, “Rotating Detonation Engine Implementation into an Open-Loop T63 Gas Turbine Engine”, 55th AIAA Aerospace Sciences Meeting, 9-13 Jan 2017.
[3] R. Huff, M. D. Polanka, M. J. McClearn, F. R. Schauer, M. L. Fotia, and J. L. Hoke, “A Disk Rotating Detonation Engine Part 1: Design and Buildup”, 56th AIAA Aerospace Sciences Meeting, 8-12 Jan 2018.
[4] M. J. McClearn, F. R. Schauer, R. Huff, M. Polanka, J. L. Hoke, and M. Fotia, “A Disk Rotating Detonation Engine Part 2: Operation” 56th AIAA Aerospace Sciences Meeting, 8-12 Jan 2018.
[5] Daniel E. Paxson and Kenji Miki, “Computational Assessment of Inlet Backflow Effects on Rotating Detonation Engine Performance and Operability”, AIAA SCITECH 2022 Forum, January 3-7, 2022, San Diego, CA & Virtual.
[6] K. Shimizu, H. Hibi, M. Koshi, M. Morii, and N. Tsuboi, “Updated Kinetic Mechanism for High-Pressure Hydrogen Combustion”, Journal of Propulsion and Power, Vol. 27, 383-395 2011.
[7] J. S. Shuen, “Upwind differencing and lu factorization for chemical non-equilibrium Navier-stokes equations,” Journal of Computational Physics, 99, 233-250, 1992.
[8] E.F. Toro, M. Spruce, W. Spears, “Restoration of the Contact Surface in the HLL-Riemann Solver," Shock Waves, 4, 25-34, 1994.
[9] S. Gottlieb, and C. W. Shu, “Total variation diminishing Runge-Kutta schemes”, Mathematics of Computation of the American Mathematical Society, 67 (221), 73-85, 1998.
[10] E.Bach, C.O. Paschereit, P. Stathopoulos, M.D. Bohon, “Advancement of Empirical Model for Predicting Stagnation Pressure Gain in Rotating Detonation Combustors”, AIAA SciTech 2022 Forum, January 3-7, 2022, San Diego, CA & Virtual.
[11] A.K.Hayashi, T.Ito, N.Tsuboi, K.Ozawa, Y.Otsuka, K.Ishii, “Numerical Analysis on Pressure Gain Combustion of Radial-Rotating Detonation Engine”, ICNC 2024, May 7-10, 2024, Kyoto, Japan.